Physics Letters A 447 (2022) 128300

Contents lists available at ScienceDirect

Physics Letters A

www.elsevier.com/locate/pla

Indefinite causal order for quantum metrology with quantum thermal noise

François Chapeau-Blondeau

Laboratoire Angevin de Recherche en Ingénierie des Systèmes (LARIS), Université d'Angers, 62 avenue Notre Dame du Lac, 49000 Angers, France

ARTICLE INFO

Article history:
Received 15 April 2022
Received in revised form 4 June 2022
Accepted 1 July 2022
Available online 8 July 2022
Communicated by M.G.A. Paris

Keywords:
Indefinite causal order
Quantum metrology
Quantum estimation
Quantum noise
Switched quantum channel

ABSTRACT

A switched quantum channel with indefinite causal order is studied for the fundamental metrological task of phase estimation on a qubit unitary operator affected by quantum thermal noise. Specific capabilities are reported in the switched channel with indefinite order, not accessible with conventional estimation approaches with definite order. Phase estimation can be performed by measuring the control qubit alone, although it does not actively interact with the unitary process – only the probe qubit doing so. Also, phase estimation becomes possible with a fully depolarized input probe or with an input probe aligned with the rotation axis of the unitary, while this is never possible with conventional approaches. The present study extends to thermal noise, investigations previously carried out with the more symmetric and isotropic qubit depolarizing noise, and it contributes to the timely exploration of properties of quantum channels with indefinite causal order relevant to quantum signal and information processing.

1. Introduction

Quantum channels arranged in indefinite causal order represent novel architectures for combining quantum processes, which exhibit specific properties useful to quantum signal and information processing, and not accessible with conventional associations with definite causal order. The principle of quantum channels with indefinite causal order has been analyzed in [1,2], and their physical implementation is discussed for instance in [2–7]. Quantum channels with indefinite causal order have been shown profitable in various tasks of quantum information processing, such as communication over noisy quantum channels [8–11], or quantum channel discrimination [12,13]. For quantum metrology, which will be the principal concern of the present study, channels with indefinite order have been studied in [14–17], to estimate the level of a qudit depolarizing noise in [14] or the temperature of a qubit thermal noise in [15], or to extract information about average displacements in a quantum system with continuous variables in [16]. The study of [17] addresses the reference task of quantum metrology consisting in quantum phase estimation in the presence of noise. Phase estimation is a fundamental task of quantum metrology, useful to many applications related to high-sensitivity and high-precision physical measurements [18–23]. For qubit phase estimation in the presence of a qubit depolarizing noise, Ref. [17] demonstrates various capabilities afforded by a switched quantum channel with indefinite causal order, and that are not accessible with standard estimation approaches with definite order. In the present study, we will address the same type of switched quantum channels with indefinite causal order involved in a task of phase estimation, as in [17]. While [17] considers phase estimation in the presence of a unital qubit depolarizing noise showing high symmetry and isotropy, we will extend the analysis here to a less regular nonunital quantum noise under the form of a qubit thermal noise, which represents also a noise of high practical relevance [24–28]. The present report provides the first analysis of a switched quantum channel with indefinite causal order for quantum phase estimation in the presence of thermal noise. It contributes to the inventory and appreciation of specific properties of quantum channels with indefinite causal order bearing relevance to quantum signal and information processing.

E-mail address: chapeau@univ-angers.fr.

https://doi.org/10.1016/j.physleta.2022.128300
0375-9601/

2. Controlled switch of two quantum channels

We consider here, as in Refs. [2,8,17], two quantum channels (1) and (2), respectively characterized by the Kraus operators $\{\mathsf{K}_k^{(1)}\}$ and $\{\mathsf{K}_k^{(2)}\}$, and which are switched between the two causal orders (1)–(2) or (2)–(1) according to the state $|0_c\rangle$ or $|1_c\rangle$ or a control qubit, as represented in Fig. 1.

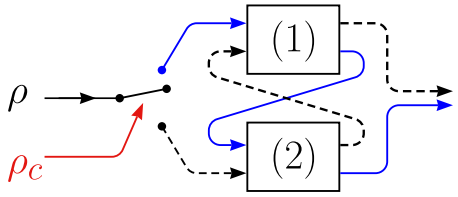

Fig. 1. According to the state ρ_c of a control qubit, the two quantum channels (1) and (2) can be cascaded in the causal order (1)–(2) (solid path) or (2)–(1) (dashed path) to affect the probe signal in state ρ.

A switched quantum channel results, which is characterized [2,8,17] by the Kraus operators

$$\mathsf{K}_{jk} = \mathsf{K}_j^{(2)}\mathsf{K}_k^{(1)} \otimes |0_c\rangle\langle 0_c| + \mathsf{K}_k^{(1)}\mathsf{K}_j^{(2)} \otimes |1_c\rangle\langle 1_c| \, . \tag{1}$$

With a control qubit placed in the general state represented by the density operator ρ_c, the switched quantum channel of Fig. 1 realizes the bipartite transformation

$$\mathcal{S}(\rho \otimes \rho_c) = \sum_j \sum_k \mathsf{K}_{jk}(\rho \otimes \rho_c)\mathsf{K}_{jk}^\dagger \, . \tag{2}$$

An interesting possibility is to place the control qubit in a coherent superposition of its two basis states, reading $|\psi_c\rangle = \sqrt{p_c}|0_c\rangle + \sqrt{1-p_c}|1_c\rangle$, with $p_c \in [0,1]$. In this way, the switched channel of Fig. 1 realizes a coherent superposition of the two alternative causal orders (1)–(2) and (2)–(1), implementing a switched quantum channel with indefinite causal order. In the general case of a control qubit with density operator ρ_c, pure or mixed, the transformation of Eq. (2) can be developed [17] into

$$\begin{aligned}\mathcal{S}(\rho \otimes \rho_c) = {} & \mathcal{S}_{00}(\rho) \otimes \langle 0_c|\rho_c|0_c\rangle |0_c\rangle\langle 0_c| + \mathcal{S}_{01}(\rho) \otimes \langle 0_c|\rho_c|1_c\rangle |0_c\rangle\langle 1_c| \\ & + \mathcal{S}_{01}^\dagger(\rho) \otimes \langle 1_c|\rho_c|0_c\rangle |1_c\rangle\langle 0_c| + \mathcal{S}_{11}(\rho) \otimes \langle 1_c|\rho_c|1_c\rangle |1_c\rangle\langle 1_c| \, .\end{aligned} \tag{3}$$

In Eq. (3), the superoperators $\mathcal{S}_{00}(\rho)$ and $\mathcal{S}_{11}(\rho)$ respectively describe transmission by the standard cascades (1)–(2) and (2)–(1), defined by the two sets of Kraus operators $\{\mathsf{K}_j^{(2)}\mathsf{K}_k^{(1)}\}$ and $\{\mathsf{K}_k^{(1)}\mathsf{K}_j^{(2)}\}$. With the pure state $\rho_c = |\psi_c\rangle\langle\psi_c|$, at $p_c = 0$ or $p_c = 1$ there is no genuine superposition of causal orders, and the operation of the switched channel in Eq. (3) reduces to these standard cascades (1)–(2) or (2)–(1), via $\mathcal{S}_{00}(\rho)$ or $\mathcal{S}_{11}(\rho)$. By contrast in Eq. (3), the superoperator

$$\mathcal{S}_{01}(\rho) = \sum_j \sum_k \mathsf{K}_j^{(2)}\mathsf{K}_k^{(1)}\rho\mathsf{K}_j^{(2)\dagger}\mathsf{K}_k^{(1)\dagger} \, , \tag{4}$$

specifically conveys the effect of the superposition of causal orders, especially acting with $\rho_c = |\psi_c\rangle\langle\psi_c|$ when $p_c \neq 0$ and $p_c \neq 1$.

We will now specifically investigate the situation where the two superposed channels (1) and (2) in Fig. 1 are formed by a unitary qubit channel affected by quantum noise, to be involved in the fundamental metrological task of phase estimation on the unitary. For such a scenario of phase estimation in a switched quantum channel with indefinite causal order, [17] studied the case of the unital isotropic depolarizing noise, while here we will investigate the case of a nonunital and less symmetric thermal noise, having also great practical relevance for the qubit [24–28].

3. A switched qubit unitary channel with thermal noise

We will examine a noisy quantum channel consisting in a qubit unitary operator U_ξ affected by a qubit noise $\mathcal{N}(\cdot)$ as represented in Fig. 2.

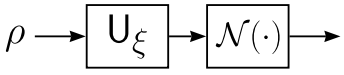

Fig. 2. Quantum channel formed by a qubit unitary operator U_ξ affected by a qubit noise $\mathcal{N}(\cdot)$, and as a whole providing a realization for channel (1) or (2) involved in Fig. 1.

The quantum channel of Fig. 2 acts on a probe qubit with input density operator

$$\rho = \begin{bmatrix} \rho_{00} & \rho_{01} \\ \rho_{01}^* & 1-\rho_{00} \end{bmatrix} = \frac{1}{2}\left(\mathrm{I}_2 + \vec{r}\cdot\vec{\sigma}\right) , \tag{5}$$

with in particular $\rho_{00} \in [0,1]$. In Eq. (5), I_2 is the identity operator on the two-dimensional qubit space $\mathcal{H}_2$, and $\vec{\sigma}$ is the formal vector of the three Pauli operators $[\sigma_x, \sigma_y, \sigma_z] = \vec{\sigma}$. The Bloch vector $\vec{r} \in \mathbb{R}^3$ is with norm $\|\vec{r}\,\| = 1$ for a pure state, and $\|\vec{r}\,\| < 1$ for a mixed state.

The qubit unitary operator U_ξ of Fig. 2 receives [29] the general parameterization

$$\mathsf{U}_\xi = \exp\left(-i\frac{\xi}{2}\vec{n}\cdot\vec{\sigma}\right), \tag{6}$$

with $\vec{n}=[n_x,n_y,n_z]^\top$ a unit vector of $\mathbb{R}^3$, and ξ a phase angle in $[0,2\pi)$ which is often a parameter of metrological interest. The unitary implements the transformation $\rho\mapsto \mathsf{U}_\xi\rho\mathsf{U}_\xi^\dagger$, equivalent to transforming the Bloch vector of the qubit by $\vec{r}\mapsto U_\xi\vec{r}$ with U_ξ (in italic) the 3×3 rotation matrix of $\mathbb{R}^3$ of angle ξ around the axis $\vec{n}$.

The quantum noise $\mathcal{N}(\cdot)$ of Fig. 2 is taken here as a generalized amplitude damping noise or quantum thermal noise, defined [29] by the four Kraus operators

$$\Lambda_1=\sqrt{p}\begin{bmatrix}1&0\\0&\sqrt{1-\gamma}\end{bmatrix}, \tag{7}$$

$$\Lambda_2=\sqrt{p}\begin{bmatrix}0&\sqrt{\gamma}\\0&0\end{bmatrix}, \tag{8}$$

$$\Lambda_3=\sqrt{1-p}\begin{bmatrix}\sqrt{1-\gamma}&0\\0&1\end{bmatrix}, \tag{9}$$

$$\Lambda_4=\sqrt{1-p}\begin{bmatrix}0&0\\\sqrt{\gamma}&0\end{bmatrix}. \tag{10}$$

On the qubit density operator ρ of Eq. (5), the noise implements the (nonunitary) transformation $\rho\mapsto\mathcal{N}(\rho)=\sum_{j=1}^4\Lambda_j\rho\Lambda_j^\dagger$ reading

$$\mathcal{N}(\rho)=\begin{bmatrix}(1-\gamma)\rho_{00}+p\gamma & \sqrt{1-\gamma}\,\rho_{01}\\ \sqrt{1-\gamma}\,\rho_{01}^* & (1-\gamma)(1-\rho_{00})+(1-p)\gamma\end{bmatrix}, \tag{11}$$

equivalent to transforming the Bloch vector of the qubit by

$$\vec{r}\longmapsto A\vec{r}+\vec{c}=\begin{bmatrix}\sqrt{1-\gamma}&0&0\\0&\sqrt{1-\gamma}&0\\0&0&1-\gamma\end{bmatrix}\vec{r}+\begin{bmatrix}0\\0\\(2p-1)\gamma\end{bmatrix}. \tag{12}$$

Such noise offers a model [29,26] to describe the coupling of the qubit with an uncontrolled environment consisting in a thermal bath at temperature T. The damping factor $\gamma\in[0,1]$ can be related to the interaction time t of the qubit with the bath as $\gamma=1-e^{-t/\tau_1}$, with τ_1 a relaxation time for the interaction. At long time $t\gg\tau_1$, one has $\gamma\to 1$ and a qubit relaxing to the equilibrium or thermalized mixed state $\rho_\infty=p|0\rangle\langle 0|+(1-p)|1\rangle\langle 1|$ having Bloch vector $\vec{r}_\infty=[0,0,2p-1]^\top$. At equilibrium, the probability is p for measuring the qubit in the ground state $|0\rangle$ and $1-p$ for measuring it in the excited state $|1\rangle$. With the energies E_0 and $E_1>E_0$ respectively for the states $|0\rangle$ and $|1\rangle$, the equilibrium probability p is given by the Boltzmann distribution as

$$p=\frac{1}{1+\exp[-(E_1-E_0)/(k_BT)]}. \tag{13}$$

By Eq. (13), the probability p characterizing the quantum thermal noise of Eqs. (7)–(12), is determined by the temperature T of the bath. From Eq. (13), the probability p decreases as the temperature T increases. A temperature $T=0$ gives a probability $p=1$ for the ground state $|0\rangle$, while at $T\to\infty$ the ground state $|0\rangle$ and excited state $|1\rangle$ become equiprobable with $p=1/2$. Therefore, from Eq. (13), when the temperature T monotonically increases from 0 to ∞, the probability p monotonically decreases from 1 to 1/2. For the sequel, as in [30], it will be convenient to refer to an effective or reduced noise temperature $T_p=2(1-p)$, which, according to Eq. (13), is a monotonically increasing function of the physical temperature T, for any value of the energy gap $E_1-E_0>0$. When $T=0$ then $p=1$ and $T_p=0$, while when $T=\infty$ then $p=1/2$ and $T_p=1$. So a physical temperature T increasing from 0 to ∞ is monotonically mapped into an effective temperature T_p increasing from 0 to 1. This provides a convenient finite range of $T_p\in[0,1]$ to convey the impact of the physical temperature $T\in[0,\infty[$, and also releases the quantitative analysis from the unimportant specific value of the energy gap $E_1-E_0>0$.

The quantum channel resulting in Fig. 2 is therefore defined by the four Kraus operators $\mathsf{K}_j=\Lambda_j\mathsf{U}_\xi$, for $j=1$ to 4. It implements the transformation $\rho\mapsto\sum_{j=1}^4\Lambda_j\mathsf{U}_\xi\rho\mathsf{U}_\xi^\dagger\Lambda_j^\dagger$, equivalent to transforming the Bloch vector of the qubit by $\vec{r}\mapsto AU_\xi\vec{r}+\vec{c}$. Two such identical noisy unitary channels as in Fig. 2 are employed to realize channels (1) and (2) in the switched quantum channel of Fig. 1. Two identical channels (1) and (2) in Fig. 1 give $\mathcal{S}_{00}(\rho)=\mathcal{S}_{11}(\rho)$ and $\mathcal{S}_{01}^\dagger(\rho)=\mathcal{S}_{01}(\rho)$ in Eq. (3). These superoperators are completely determined by the four Kraus operators $\mathsf{K}_j=\Lambda_j\mathsf{U}_\xi$. In particular, the superoperators $\mathcal{S}_{00}(\rho)$ and $\mathcal{S}_{11}(\rho)$ describe the (identical) action on the probe qubit ρ of the standard cascades (1)–(2) and (2)–(1), expressible as $\mathcal{S}_{00}(\rho)=\mathcal{S}_{11}(\rho)=\sum_{j=1}^4\sum_{k=1}^4\Lambda_j\mathsf{U}_\xi\Lambda_k\mathsf{U}_\xi\rho\mathsf{U}_\xi^\dagger\Lambda_k^\dagger\mathsf{U}_\xi^\dagger\Lambda_j^\dagger$, equivalently performing the Bloch vector transformation $\vec{r}\mapsto AU_\xi\left(AU_\xi\vec{r}+\vec{c}\right)+\vec{c}$. Meanwhile, the superoperator $\mathcal{S}_{01}(\rho)$ following from Eq. (4) with $\mathsf{K}_j^{(1)}=\mathsf{K}_j^{(2)}=\Lambda_j\mathsf{U}_\xi$, is responsible for the distinctive properties stemming from the indefinite superposition of causal orders, as we are going to see in more detail.

4. Measurement for estimation

We want to exploit the switched channel to perform parameter estimation, chiefly of the phase ξ of the unitary U_ξ, but possibly also of the parameters p or γ of the qubit thermal noise. For this objective, it is possible to measure the two qubits – probe and control – delivered at the output of the switched channel in the joint state $\mathcal{S}(\rho\otimes\rho_c)$ from Eq. (3). A simpler approach would be to measure only the probe qubit, since it is the qubit that interacts with the process U_ξ and noise $\mathcal{N}(\cdot)$. If at the same time the control qubit is discarded (unobserved), the measurement on the probe qubit is ruled by the reduced density operator obtained by partially tracing the joint state $\mathcal{S}(\rho\otimes\rho_c)$ of Eq. (3) over the control qubit. It results as $\rho^{\rm prob}=\mathrm{tr}_{\rm control}\big[\mathcal{S}(\rho\otimes\rho_c)\big]=\mathcal{S}_{00}(\rho)$, which is nothing else than the density operator of a single probe qubit that would have traversed the standard cascade (1)–(2) or (2)–(1), with no effect from the superposition of causal orders. An interesting alternative, manifesting the specific and useful properties stemming from the superposition of causal orders, is to choose to measure the control qubit alone while discarding the probe qubit. In this circumstance, the measurement on the control qubit is ruled by the reduced density operator obtained by partially tracing the joint state $\mathcal{S}(\rho\otimes\rho_c)$ of Eq. (3) over the probe qubit. It results as $\rho^{\rm con}=\mathrm{tr}_{\rm probe}\big[\mathcal{S}(\rho\otimes\rho_c)\big]$, yielding when the control qubit is initialized in the pure state $|\psi_c\rangle=\sqrt{p_c}|0_c\rangle+\sqrt{1-p_c}|1_c\rangle$,

$$\rho^{\rm con}=p_c|0_c\rangle\langle 0_c|+(1-p_c)|1_c\rangle\langle 1_c|+Q_c\sqrt{(1-p_c)p_c}\Big(|1_c\rangle\langle 0_c|+|0_c\rangle\langle 1_c|\Big)\,, \tag{14}$$

since $\mathcal{S}_{00}(\rho)$ is a qubit density operator giving $\mathrm{tr}[\mathcal{S}_{00}(\rho)]=1$, and where we have defined the factor

$$Q_c=\mathrm{tr}\big[\mathcal{S}_{01}(\rho)\big]\,. \tag{15}$$

A very interesting feature is that this factor Q_c in Eq. (15) is in general dependent on the properties of both the unitary U_ξ and the thermal noise $\mathcal{N}(\cdot)$, as we are going see in more detail below. This means that the control qubit alone can be measured at the output of the switched channel, while discarding the probe qubit, and in this way extract information about the probed processes U_ξ and $\mathcal{N}(\cdot)$. This is remarkable since the control qubit does not interact with the probed processes U_ξ and $\mathcal{N}(\cdot)$, only the probe qubit does so. Nevertheless, the type of coupling induced by the switched channel with indefinite causal order, as conveyed by Eq. (3), transfers information from the probed processes U_ξ and $\mathcal{N}(\cdot)$ to the control qubit.

To quantify the performance of the control qubit, for a task of parameter estimation, a generally meaningful criterion is the quantum Fisher information, contained in the state $\rho^{\rm con}$, about some parameter of interest probed in the switched channel [31–34]. The quantum Fisher information stands as an upper bound to the classical Fisher information, which in turn determines the smallest mean-squared error that can be achieved in the estimation. In this way, the quantum Fisher information is a fundamental criterion characterizing the best performance that can be envisaged, applying equally to any estimation strategies, and in this respect dispensing to refer to an explicit quantum measurement and an explicit estimator. We will concentrate here on estimating the phase ξ of the noisy unitary process U_ξ, which is often a parameter of prime interest in quantum metrology. Nevertheless, a comparable analysis would hold equally for estimating other parameters, such as the probability p or the damping factor γ of the thermal noise. Based on [17], when measuring the control qubit of the switched channel in the state $\rho^{\rm con}$ of Eq. (14), the quantum Fisher information for estimating the phase ξ follows as

$$F_q^{\rm con}(\xi)=4(1-p_c)p_c\frac{\big[\partial_\xi Q_c(\xi)\big]^2}{1-Q_c^2(\xi)}\,, \tag{16}$$

involving the derivative $\partial_\xi Q_c(\xi)\equiv\partial Q_c(\xi)/\partial\xi$ of the factor $Q_c\equiv Q_c(\xi)$ from Eq. (15) seen as a function of ξ and characterizing the measured state $\rho^{\rm con}$ of Eq. (14). This quantum Fisher information in Eq. (16) is maximized for a control qubit prepared with the probability $p_c=1/2$, i.e. with a maximally indefinite order via an even superposition of the two orders (1)–(2) and (2)–(1) in Fig. 1, so as to give at $p_c=1/2$,

$$F_q^{\rm con}(\xi)=\frac{\big[\partial_\xi Q_c(\xi)\big]^2}{1-Q_c^2(\xi)}\,. \tag{17}$$

We essentially focus the analysis on this optimal configuration at $p_c=1/2$ in the sequel.

For a meaningful example that illustrates essential distinctive properties accessible with the control qubit of the switched channel, while remaining analytically tractable with closed-form expressions of moderate size to handle, we consider the situation of a unitary U_ξ in Eq. (6) with axis $\vec{n}=[0,0,1]^\top=\vec{e}_z$. The four Kraus operators $\mathsf{K}_j=\Lambda_j\mathsf{U}_\xi$ then follow to determine the two-qubit joint state $\mathcal{S}(\rho\otimes\rho_c)$ of Eq. (3), which is explicitly worked out in the Appendix. We also obtain in the Appendix the characterization of the operator $\mathcal{S}_{01}(\rho)$ whose trace is computed according to Eq. (15) to yield

$$Q_c(\xi)=2\gamma\sqrt{1-\gamma}\Big[(1-2p)\rho_{00}+p\Big]\cos(\xi)+(2-\gamma)\gamma(2p-1)\rho_{00}+(1-\gamma p)^2\,. \tag{18}$$

The term $\rho_{00}\in[0,1]$ in Eq. (18) conveys the influence from the initial preparation in Eq. (5) of the input probe qubit. Follows the derivative

$$\partial_\xi Q_c(\xi)=-2\gamma\sqrt{1-\gamma}\Big[(1-2p)\rho_{00}+p\Big]\sin(\xi)\,, \tag{19}$$

providing a complete determination of the quantum Fisher information $F_q^{\rm con}(\xi)$ of Eq. (17).

For comparison, a meaningful reference is the quantum Fisher information $F_q(\xi)$ accessible for estimating the phase ξ when directly measuring the output qubit of a single standard channel as in Fig. 2. For an input probe qubit with Bloch vector $\vec{r}$ as in Eq. (5), we have for instance from [35] the expression

$$F_q(\xi) = \frac{\left[(AU_\xi\vec{r}+\vec{c})A(\vec{n}\times U_\xi\vec{r})\right]^2}{1-(AU_\xi\vec{r}+\vec{c})^2} + \left[A(\vec{n}\times U_\xi\vec{r})\right]^2 . \tag{20}$$

The conditions for maximizing the quantum Fisher information $F_q(\xi)$ of Eq. (20) are analyzed for instance in [22,35]. With the thermal noise model of Eqs. (7)–(12), the quantum Fisher information $F_q(\xi)$ of Eq. (20) for the standard channel of Fig. 2, can reach the overall maximum value $F_q^{\max}(\xi) = 1-\gamma$ when three conditions are satisfied [22,35]: (i) the input probe must be pure with $\|\vec{r}\,\| = 1$; (ii) the Bloch vector $\vec{r}$ defining the input probe must be orthogonal to the rotation axis $\vec{n}$ of the unitary U_ξ under estimation; (iii) the vector $\vec{n}\times U_\xi\vec{r}$ in Eq. (20) must be orthogonal to the Oz axis of $\mathbb{R}^3$ set by the thermal noise of Eq. (12). This usually implies a ξ-dependent condition on the rotated probe $U_\xi\vec{r}$, that usually cannot be met by a fixed input probe $\vec{r}$, but can be circumvented by adaptively adjusting the input probe in an iterative estimation protocol [36,37]. When gradually departing from these conditions, the Fisher information $F_q(\xi)$ gradually decays below the maximum $F_q^{\max}(\xi) = 1-\gamma$. Especially, when the input probe $\vec{r}$ tends to align with the axis $\vec{n}$, or when it depolarizes as $\|\vec{r}\,\| \to 0$, then $F_q(\xi)$ goes to zero and phase estimation from the standard channel of Fig. 2 becomes completely inoperative. Standard phase estimation resting on the same elementary probe–unitary interaction $\rho \mapsto \mathsf{U}_\xi\rho\mathsf{U}_\xi^\dagger$ will remain inoperative in the same conditions, even with more elaborate scenarios as with several passes through U_ξ of the probe or several probing qubits possibly entangled [38,17].

By contrast, a distinctive feature is that the control qubit of the switched channel exhibits a Fisher information $F_q^{\mathrm{con}}(\xi)$ in Eq. (17) not limited in the same way by the conditions (i)–(iii) above. In this respect, the control qubit gives access to novel capabilities relevant to phase estimation and complementary to those offered by the standard approach of Eq. (20). Especially, the performance of the control qubit for phase estimation, as assessed by the Fisher information $F_q^{\mathrm{con}}(\xi)$ of Eq. (17), is not adversely impacted by ill configurations of the input probe $\vec{r}$ of Eq. (5) in relation to the rotation axis $\vec{n}$. Even when $\vec{r}\,/\!/\,\vec{n}$ with an input probe $\vec{r}$ parallel to the rotation axis $\vec{n}$, or when $\|\vec{r}\,\| = \vec{0}$ with a fully depolarized input probe, the control qubit of the switched channel remains operative for phase estimation. We specially focus in the sequel on analyzing the performance of the control qubit for phase estimation in these conditions where standard phase estimation becomes completely inoperative, with $F_q(\xi) \equiv 0$ in Eq. (20).

Figs. 3 to 6 illustrate the impact of the thermal noise parameters on the performance $F_q^{\mathrm{con}}(\xi)$ of the control qubit of the switched channel for phase estimation, in conditions where standard phase estimation is completely inoperative.

Figs. 3 and 4 deal with two cases of a pure input probe, $\rho = |0\rangle\langle 0|$ associated with $\rho_{00} = 1$ in Fig. 3, and $\rho = |1\rangle\langle 1|$ associated with $\rho_{00} = 0$ in Fig. 4. In both cases the input Bloch vector $\vec{r}$ is parallel to the rotation axis $\vec{n} = \vec{e}_z$. In this circumstance, for the standard

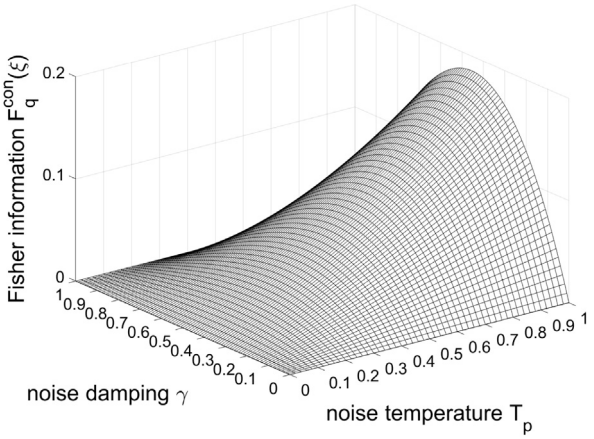

Fig. 3. For the control qubit of the switched channel, quantum Fisher information $F_q^{\mathrm{con}}(\xi)$ of Eq. (17), for a phase $\xi = \pi/4$, as a function of the effective temperature $T_p = 2(1-p)$ and damping factor γ of the quantum thermal noise of Eqs. (7)–(12). The input probe is prepared in the pure state $\rho = |0\rangle\langle 0|$ with Bloch vector $\vec{r} = \vec{e}_z$ parallel to the rotation axis $\vec{n} = \vec{e}_z$ of the unitary U_ξ, making standard phase estimation completely inoperative.

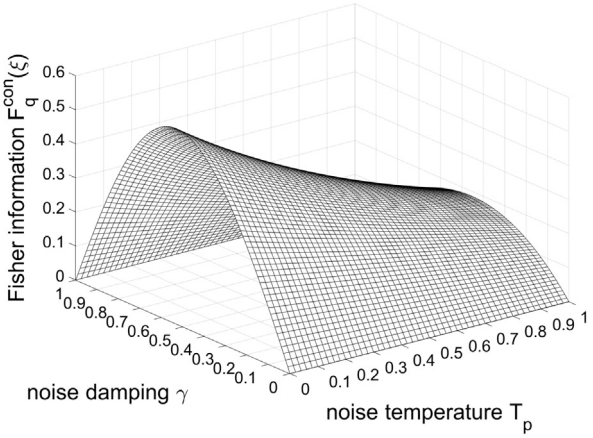

Fig. 4. Same as in Fig. 3, except that the input probe is prepared in the pure state $\rho = |1\rangle\langle 1|$ with Bloch vector $\vec{r} = -\vec{e}_z$ parallel to the rotation axis $\vec{n} = \vec{e}_z$ of the unitary U_ξ, also making standard phase estimation completely inoperative.

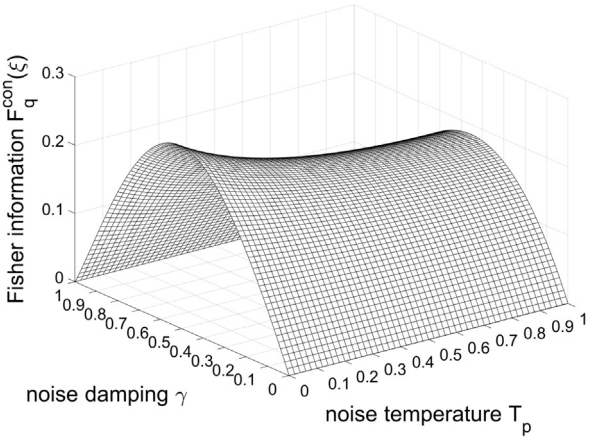

Fig. 5. Same as in Fig. 3, except that the input probe is prepared in the fully depolarized mixed state $\rho = I_2/2$ with Bloch vector $\vec{r} = \vec{0}$, where standard phase estimation is also completely inoperative.

estimation the Fisher information $F_q(\xi)$ of Eq. (20) vanishes since $U_\xi \vec{r} \,/\!/\, \vec{n}$, manifesting the impossibility of estimating the phase by measuring the probe qubit. By contrast, the control qubit of the switched channel remains efficient for estimation, as manifested by a nonvanishing Fisher information $F_q^{con}(\xi)$ in Figs. 3–4.

In addition, Figs. 3–4 illustrate two typical behaviors accessible to the Fisher information $F_q^{con}(\xi)$ of Eq. (17), and therefrom to the estimation efficiency, upon increasing the temperature of the thermal bath, at any fixed value of the damping factor γ. Depending on the input probe ρ, Fig. 3 shows the possibility of a Fisher information $F_q^{con}(\xi)$ that increases as the noise temperature T_p increases, while Fig. 4 shows a decreasing $F_q^{con}(\xi)$. This manifests that the (thermal) noise is not univocally detrimental to the estimation efficiency from the switched channel, as also observed in [17] with depolarizing noise. Increasing the level of noise, via increasing the noise temperature in Fig. 3, may enhance the Fisher information $F_q^{con}(\xi)$ and therefore the efficiency of the control qubit for the phase estimation. Such a versatile role of noise in the switched channel can also be substantiated in the following way. In the elementary noisy unitary channel of Fig. 2, the noise $\mathcal{N}(\cdot)$ has the natural effect of degrading the probe qubit, and hence the estimation efficiency. Yet, when two such channels are superposed as in Fig. 1, the noise is necessary to make the two superposed channels (1) and (2) distinguishable, and to couple the control qubit to the unitary U_ξ. At vanishing noise, the two channels (1) and (2) are two identical unitary channels with one single Kraus operator $K_1 = U_\xi$, so that the joint probe-control output state of Eq. (3) reduces to the separable state $\mathcal{S}(\rho \otimes \rho_c) = \mathcal{S}_{00}(\rho) \otimes |\psi_c\rangle\langle\psi_c|$, and the control qubit does not couple to the unitary U_ξ. This in particular entails, at vanishing noise, when the damping $\gamma \to 0$ in Eq. (12), a coupling factor $Q_c(\xi)$ in Eq. (18) which becomes independent of the phase ξ, so that the control qubit cannot serve to estimate the phase ξ. A nonvanishing amount of noise is required to couple the control qubit to the phase ξ and maintain a ξ-dependent $Q_c(\xi)$ in Eq. (18). Increasing the amount of noise, in this way, may be beneficial to the efficiency of the control qubit for estimation, depending on the conditions, as determined by the expression of Eq. (17) for the quantum Fisher information $F_q^{con}(\xi)$.

Fig. 5 shows the situation of a fully depolarized input probe $\rho = I_2/2$ with $\rho_{00} = 1/2$ and Bloch vector $\vec{r} = \vec{0}$, which maintains a nonvanishing Fisher information $F_q^{con}(\xi)$ in Eq. (17) and therefore the capability of the control qubit of the switched channel for estimating the phase ξ. On the contrary, with the standard channel of Fig. 2, a fully depolarized input probe $\rho = I_2/2$ on the unitary, undergoes the transformation $\rho = I_2/2 \mapsto U_\xi \rho U_\xi^\dagger = I_2/2$, and extracts no information about U_ξ, so that it is completely inoperative for estimating its phase ξ.

Figs. 3–5 also clearly show a non-monotonic action of the damping factor $\gamma = 1 - e^{-t/\tau_1}$ on the quantum Fisher information $F_q^{con}(\xi)$, at any fixed temperature of the thermal noise. A damping factor $\gamma = 1 - e^{-t/\tau_1}$ tending to zero at an extremely brief exposition time $t \ll \tau_1$ to the noise, is the situation of a vanishing thermal noise. As explained above, at vanishing noise the control qubit is no longer coupled to the unitary U_ξ in the switched channel, whence the vanishing Fisher information $F_q^{con}(\xi)$ at $\gamma = 0$ in Figs. 3–5. Also, when $\gamma = 1 - e^{-t/\tau_1} \to 1$, with an increasing exposition time $t \gg \tau_1$, the Fisher information $F_q^{con}(\xi)$ also tends to vanish, as visible in Figs. 3–5. This points to an intermediate damping γ, i.e. an intermediate exposition time t to the noise, to maximize the estimation efficiency $F_q^{con}(\xi)$, with t not too short so that the control qubit sufficiently couples to U_ξ, and t not too long to avoid thermalization where the process terminates in an equilibrium state independent of U_ξ. This is reflected in a Fisher information $F_q^{con}(\xi)$ of the control qubit, culminating at a maximum for an intermediate damping γ, whose precise value is slightly dependent on the temperature of the thermal bath, as observed in the finer view provided by Fig. 6 in the illustrative conditions of Fig. 4.

Such a constructive role of the thermal noise here, which may benefit to the efficiency of the control qubit for estimation, was similarly observed with the depolarizing noise in the coherently superposed channels of [17,39]. Such a constructive role of noise can be related to a phenomenon of stochastic resonance, a general effect taking place in diverse information processing operations, classical [40–43] or quantum [44–48], and where maximum efficacy is observed at a non-vanishing optimal amount of noise. Here it confirms with a novel scenario that quantum noise or decoherence can sometimes turn beneficial to quantum information processing.

Fig. 6 also compares the quantum Fisher information of the control qubit of the switched channel and that of the standard channel of Fig. 2 when both channels are operated at their best. When the standard channel of Fig. 2 can be operated in its optimal conditions, matching the three conditions (i)–(iii) mentioned above after Eq. (20), the maximal quantum Fisher information $F_q^{max}(\xi) = 1 - \gamma$ it obtains is usually superior to $F_q^{con}(\xi)$ from the switched channel, over a significant range of the noise parameters (p, γ). Nevertheless, as visible in Fig. 6, there exists a range, at high p and γ, where $F_q^{con}(\xi)$ from the switched channel becomes superior to $F_q^{max}(\xi) = 1 - \gamma$ from the standard channel. In the conditions of Fig. 6, as p and γ go to 1, one has for the control qubit the Fisher information $F_q^{con}(\xi) \to 2(1 - \gamma)$. The same quantum Fisher information $2(1 - \gamma) = 2F_q^{max}(\xi)$ could be reached by two independent qubits traversing the standard channel

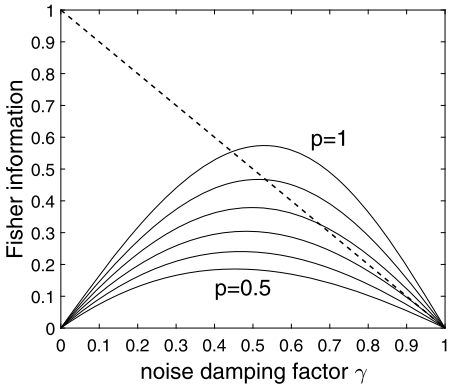

Fig. 6. Solid lines: in the conditions of Fig. 4, the quantum Fisher information $F_q^{\rm con}(\xi)$ of Eq. (17) as a function of the noise damping factor γ, for 6 values of the probability p fixed by the noise temperature: the uppermost curve is for $p=1$ at zero temperature, then in descending order of the curves are $p=0.9$, 0.8, 0.7 and 0.6, finally the lowermost curve is for $p=0.5$ at infinite temperature. Dashed curve: maximal quantum Fisher information $F_q^{\rm max}(\xi)=1-\gamma$ accessible in Eq. (20) with the standard channel of Fig. 2 operated in its optimal conditions with an input probe prepared in the pure state $|+\rangle$ with Bloch vector $\vec{r}=\vec{e}_x$.

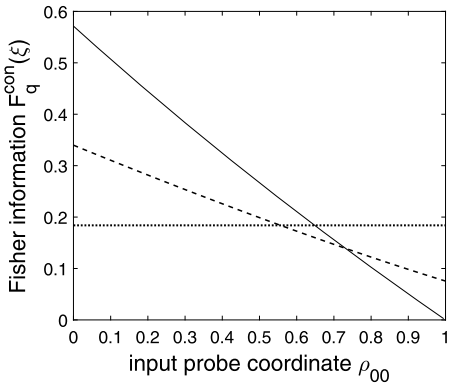

Fig. 7. Quantum Fisher information $F_q^{\rm con}(\xi)$ of Eq. (17), for a phase $\xi=\pi/4$, as a function of the input probe coordinate ρ_{00}, with a noise damping factor $\gamma=0.5$ and a noise probability $p=1$ corresponding to the zero temperature $T=0$ (solid line), $p=0.75$ at intermediate temperature T (dashed line), $p=0.5$ at infinite temperature $T=\infty$ (dotted line). The pure input probe $\rho=|1\rangle\langle 1|$ is at $\rho_{00}=0$, while $\rho=|0\rangle\langle 0|$ is at $\rho_{00}=1$, the fully depolarized input probe $\rho={\rm I}_2/2$ is at $\rho_{00}=1/2$, all three configurations where standard phase estimation is completely inoperative.

of Fig. 2 and then being measured. A single qubit traversing twice, in two passes, the standard channel of Fig. 2, would achieve a quantum Fisher information comparable to Eq. (20) but acting on the Bloch vector $AU_\xi\left(AU_\xi\vec{r}+\vec{c}\right)+\vec{c}$ as transformed by the two passes. Yet this would lead to a poorer performance compared with the two independent qubits, because when starting the second pass the (noisy) qubit would no longer be in the optimal input state. Two entangled probe qubits, although more complicated to handle, could even be envisaged to probe the standard channel of Fig. 2, to benefit from the so-called Heisenberg enhanced performance, but the optimal configurations in the presence of thermal noise are not fully characterized, and it is known that the Heisenberg enhanced performance is very fragile to noise [19,49,38,50]. In the high range of the noise parameters (p,γ) in Fig. 6, the control qubit of the switched channel performs as well as two independent qubits across the standard channel, but it can be measured alone. The two channels compared in Fig. 6 are rather distinct in their constitution and mode of operation, means and resources they imply. The standard channel which is more directly intended for estimation, however, does not always achieve the best performance of the two channels. The two channels are rather complementary, especially as the switched channel offers estimation capabilities inaccessible to the standard channel and forming the main focus of this study.

Fig. 7 shows typical evolutions of the quantum Fisher information $F_q^{\rm con}(\xi)$ resulting from Eq. (17) and Eqs. (18)–(19) for the control qubit of the switched channel, as a function of the coordinate ρ_{00} of the input probe ρ.

The configurations in Fig. 7 encompass the pure input probes $\rho=|1\rangle\langle 1|$ at $\rho_{00}=0$ and $\rho=|0\rangle\langle 0|$ at $\rho_{00}=1$, the fully depolarized input probe $\rho={\rm I}_2/2$ at $\rho_{00}=1/2$, all three configurations where standard phase estimation is completely inoperative. Meanwhile, in these configurations, and over the whole range of $\rho_{00}\in[0,1]$, the control qubit of the switched channel generally remains operative for estimating the phase ξ, as established by the nonvanishing Fisher information $F_q^{\rm con}(\xi)$ in Fig. 7. When seen as a function of ρ_{00}, the Fisher information $F_q^{\rm con}(\xi)$ resulting from Eqs. (17)–(19), is a decreasing function of $\rho_{00}\in[0,1]$, so that $F_q^{\rm con}(\xi)$ is always maximized in $\rho_{00}=0$, that is, by the pure input probe $\rho=|1\rangle\langle 1|$, as in Figs. 4 and 6.

Finally, it is possible to refer to an explicit measurement of the control qubit in the state $\rho^{\rm con}$ of Eq. (14), by means of a von Neumann measurement in the Hadamard basis $\{|+\rangle,|-\rangle\}$. The two measurement outcomes of projecting the control qubit on $|+\rangle$ or $|-\rangle$ occur with the probabilities $\Pr\{|\pm\rangle\}=P_\pm^{\rm con}$ which are

$$P_\pm^{\rm con}=\langle\pm|\rho^{\rm con}|\pm\rangle=\frac{1}{2}\pm\sqrt{(1-p_c)p_c}\,Q_c\,. \tag{21}$$

This binary measurement result contains, about the unknown phase ξ, the classical Fisher information [35]

$$F_c^{\rm con}(\xi) = \frac{(\partial_\xi P_+^{\rm con})^2}{(1-P_+^{\rm con})P_+^{\rm con}} \tag{22}$$

$$= \frac{4(1-p_c)p_c\big[\partial_\xi Q_c(\xi)\big]^2}{1-4(1-p_c)p_c Q_c^2(\xi)} \,. \tag{23}$$

At the optimal preparation $p_c = 1/2$ of the control qubit, $F_c^{\rm con}(\xi)$ gets maximized at the level $F_q^{\rm con}(\xi)$ of Eq. (17). This establishes the measurement of the control qubit in the Hadamard basis $\big\{|+\rangle, |-\rangle\big\}$ as an optimal measurement, reaching the highest possible classical Fisher information $F_c^{\rm con}(\xi) = F_q^{\rm con}(\xi)$, and by means of the maximum likelihood estimator reaching the smallest mean-squared estimation error. Measurement in the Hadamard basis $\big\{|+\rangle, |-\rangle\big\}$ is equivalent to measuring the spin observable $\vec{\omega}_c \cdot \vec{\sigma}$ characterized by the measurement vector $\vec{\omega}_c = [1,0,0]^\top = \vec{e}_x$. It is remarkable that such a fixed optimal measurement reaching $F_c^{\rm con}(\xi) = F_q^{\rm con}(\xi)$ exists for the control qubit, independent of the axis $\vec{n}$ and angle ξ of the unitary U_ξ under estimation. By comparison, standard estimation approaches ruled by Eq. (20) are in general not granted with such a fixed optimal measurement, and to reach the optimum of $F_c(\xi) = F_q(\xi)$ matching the classical and quantum Fisher informations, they usually need [35] to measure a spin observable $\vec{\omega} \cdot \vec{\sigma}$ with a measurement vector $\vec{\omega}$ dependent on $\vec{n}$ and ξ, which is not generally feasible with an unknown phase ξ.

In the switched channel, the measurement in the Hadamard basis $\big\{|+\rangle, |-\rangle\big\}$ of the control qubit leaves the probe qubit in the unnormalized conditional state

$$\rho_\pm = {}_c\langle \pm | \mathcal{S}(\rho \otimes \rho_c) | \pm \rangle_c = \frac{1}{2}\mathcal{S}_{00}(\rho) \pm \sqrt{(1-p_c)p_c}\,\mathcal{S}_{01}(\rho) \,. \tag{24}$$

After proper normalization by the corresponding probabilities of occurrence $P_\pm^{\rm con} = \mathrm{tr}(\rho_\pm)$ of Eq. (21), one obtains the post-measurement state of the probe qubit $\rho_\pm^{\rm post} = \rho_\pm / P_\pm^{\rm con}$ conditioned on the measurement outcome obtained on the control qubit. It is observed that in general this state $\rho_\pm^{\rm post}$ of the probe is dependent on the phase ξ under estimation, so that the probe qubit can be subsequently measured, after the control qubit, so as to extract additional information about the phase ξ. Proceeding in this way is a sequential strategy, implementing two separable measurements, successively on the control and probe qubits. A joint entangled measurement of the qubit pair could also be envisaged, based on the explicit characterization of the joint state $\mathcal{S}(\rho \otimes \rho_c)$ developed in the Appendix. Such two-qubit strategies are a priori more complicated to analyze, to optimize and to implement. Interesting properties could nevertheless result, based on the non-standard capabilities contributed by the control qubit we reported here. This direction is open for further investigation to complement the present demonstration of non-standard capabilities offered by the control qubit of the switched channel for quantum phase estimation in presence of thermal noise.

5. Discussion and conclusion

We have considered the switched quantum channel with indefinite causal order of Fig. 1 when the elementary channels (1) and (2) are two copies of the noisy unitary qubit channel of Fig. 2. From the characterization of the two-qubit probe-control state $\mathcal{S}(\rho \otimes \rho_c)$ from Eq. (3) delivered by the switched channel, we have specifically investigated the properties accessible for the fundamental metrological task of phase estimation on the unitary process U_ξ in the presence of a quantum thermal noise $\mathcal{N}(\cdot)$. This study complements the report of [17] that concentrated on the qubit depolarizing noise, and it brings further results useful to a broader appreciation of the capabilities of switched channels with indefinite causal order for quantum metrology. We have observed here, as in [17], that the noise is an important ingredient to make the elementary channels (1) and (2) distinguishable, so that the superposition of Fig. 1 does not reduce to a standard cascade of two identical unitaries U_ξ and so that it can exhibit novel properties inaccessible to standard cascades with definite causal order.

Another important property is that in the presence of noise, the control qubit of the switched channel gets coupled to the unitary U_ξ, in such a way that the control qubit alone, although it does not actively interact with the unitary U_ξ, can be measured to estimate its phase ξ. In standard estimation approaches, such noninteracting qubits, to be of some use, need to be jointly measured with the active probing qubits [38,34]. This points here to non-standard quantum correlations induced in the switched channel with indefinite causal order, offering non-standard properties useful to quantum estimation, as also observed in [17]. We then have concentrated the analysis on such non-standard properties specific to the switched channel. Especially, we have analyzed phase estimation from the control qubit alone in configurations of the input probe where standard estimation approaches become completely inoperative, even when repeated with multiple probing qubits or several passes across the unitary U_ξ under estimation. In particular, we have shown that the control qubit remains efficient for phase estimation even with an input probe $\vec{r}$ aligned with the rotation axis $\vec{n}$ of the unitary U_ξ, or with a fully depolarized input probe.

In the present study, the probe and control qubits have different status and position, with a probe qubit that directly interacts with the noisy unitary U_ξ and a control qubit that does not. This conforms with the common reference framework for studying switched non-causal order, of two noisy channels whose causal order is driven by a noise-free control signal, as for instance in [8–15,17]. However, when the control qubit is also affected by some quantum noise or alteration, the present analysis can be used to predict how the essential properties stemming from non-causal order, as conveyed by the quantum Fisher information $F_q^{\rm con}(\xi)$, are preserved or gradually diminished. When the input state ρ_c of the control qubit is a pure state that gradually departs from the optimum pure state at $p_c = 1/2$, the quantum Fisher information $F_q^{\rm con}(\xi)$ in Eq. (16) of the control qubit gradually decays, but does not vanish until the superposition of orders completely disappears at $p_c = 0$ or $p_c = 1$. When the control state ρ_c becomes a mixed state, Eq. (3) shows that its action is still operative and conveyed by its matrix elements in the basis $\big\{|0_c\rangle, |1_c\rangle\big\}$. When tracing Eq. (3) over the probe, the matrix elements $\langle 0_c|\rho_c|1_c\rangle$ and $\langle 1_c|\rho_c|0_c\rangle = \langle 0_c|\rho_c|1_c\rangle^*$ are transported as multiplicative factors on Q_c in Eq. (14), in place of $\sqrt{(1-p_c)p_c}$ of the pure control. The factor $Q_c \equiv Q_c(\xi) = \mathrm{tr}\big[\mathcal{S}_{01}(\rho)\big]$ remains the essential element that conveys the dependence on the phase ξ of the transformed state $\rho^{\rm con}$ of the control qubit, via Eqs. (15) or (18) which are unchanged as determined by the probe qubit. As long as $\langle 0_c|\rho_c|1_c\rangle$ is not reduced to

zero, the control state $\rho^{\rm con}$ of Eq. (14) remains dependent, via $Q_c(\xi)$, on the phase ξ and can serve to its estimation. This is reflected in a quantum Fisher information $F_q^{\rm con}(\xi)$ of the control qubit that gradually decays with $|\langle 0_c|\rho_c|1_c\rangle|$, to vanish when $|\langle 0_c|\rho_c|1_c\rangle|$ reaches zero, but not earlier. As long as $\rho^{\rm con}$ remains dependent on ξ it can be measured to estimate ξ, and an additional noise altering $\rho^{\rm con}$ before it can be measured, would still preserve its capability for phase estimation, until the off-diagonal matrix elements of the control qubit state that carry $Q_c(\xi)$ are completely canceled by the noise. In this way, the properties of the control qubit for phase estimation are robustly preserved.

Other explorations can be envisaged of the properties of the switched channel with indefinite causal order, based on the general characterization of the two-qubit output state $\mathcal{S}(\rho\otimes\rho_c)$ of Eq. (3). For instance, estimation of the thermal noise parameters γ or p can be envisaged, and this can again be performed by measuring the control qubit alone, while discarding the probe qubit interacting with the thermal bath. This is feasible thanks to the coupling factor Q_c in Eq. (14) which bears dependence, as indicated by Eq. (18), also on the noise parameters γ and p and thus extract information about them. This is still true for instance with a fully depolarized input probe $\rho = {\rm I}_2/2$, having $\rho_{00} = 1/2$. Our analysis, in the special case where the phase of the unitary U_ξ is canceled as $\xi \equiv 0$, describes a pure thermal noise channel engaged in a superposition of causal orders, as studied for quantum thermometry in [15] in the thermalized regime when the damping $\gamma \to 1$. Another direction of exploration could be the investigation of extensions and generalizations proposed of structures with non-causal order [51,9,52] for estimation tasks with noise as we considered here in the quantum switch superposing two causal orders.

In this way, the present study brings additional elements and results to better appreciate the capabilities of switched quantum channels with indefinite causal order, especially with novel and specific properties, to contribute to quantum estimation and quantum metrology and more broadly to quantum signal and information processing.

CRediT authorship contribution statement

François Chapeau-Blondeau: Writing – review & editing, Writing – original draft, Validation, Supervision, Project administration, Methodology, Investigation, Formal analysis, Conceptualization.

Declaration of competing interest

The authors declare that they have no known competing financial interests or personal relationships that could have appeared to influence the work reported in this paper.

Data availability

No data was used for the research described in the article.

Appendix A

In this Appendix, we explicitly work out the joint state $\mathcal{S}(\rho\otimes\rho_c)$ of Eq. (3), as a function of the parameters (p,γ) of the thermal noise, with a control qubit prepared in the pure state $|\psi_c\rangle = \sqrt{p_c}|0_c\rangle + \sqrt{1-p_c}|1_c\rangle$, and a unitary U_ξ with axis $\vec{n} = \vec{e}_z$. The density operator $\mathcal{S}_{00}(\rho) = \sum_{j=1}^4\sum_{k=1}^4 \Lambda_j\mathsf{U}_\xi\Lambda_k\mathsf{U}_\xi\rho\mathsf{U}_\xi^\dagger\Lambda_k^\dagger\mathsf{U}_\xi^\dagger\Lambda_j^\dagger$ can be represented as the 2×2 matrix

$$\mathcal{S}_{00}(\rho) = \begin{bmatrix} (1-\gamma)^2\rho_{00} + p(1-\gamma)\gamma + p\gamma & (1-\gamma)\rho_{01}e^{-i2\xi} \\ (1-\gamma)\rho_{01}^* e^{i2\xi} & (1-\gamma)^2(1-\rho_{00}) + (1-p)(1-\gamma)\gamma + (1-p)\gamma \end{bmatrix}. \tag{A-1}$$

The Hermitian operator $\mathcal{S}_{01}(\rho) = \sum_{j=1}^4\sum_{k=1}^4 \Lambda_j\mathsf{U}_\xi\Lambda_k\mathsf{U}_\xi\rho\mathsf{U}_\xi^\dagger\Lambda_j^\dagger\mathsf{U}_\xi^\dagger\Lambda_k^\dagger$ resulting in Eq. (4) can be represented as the 2×2 matrix

$$\mathcal{S}_{01}(\rho) = \begin{bmatrix} b_{00} & b_{01} \\ b_{01}^* & b_{11} \end{bmatrix}, \tag{A-2}$$

with the matrix elements

$$b_{00} = 2\gamma\sqrt{1-\gamma}\,p(1-\rho_{00})\cos(\xi) + \big[1-\gamma(1-p)\big]^2\rho_{00}\,, \tag{A-3}$$

$$b_{01} = \big[(1-\gamma)e^{-i2\xi} + \gamma^2(1-p)p\big]\rho_{01}\,, \tag{A-4}$$

$$b_{11} = 2\gamma\sqrt{1-\gamma}(1-p)\rho_{00}\cos(\xi) + (1-\gamma p)^2(1-\rho_{00})\,. \tag{A-5}$$

We especially obtain for Eq. (15) the trace $Q_c = {\rm tr}\big[\mathcal{S}_{01}(\rho)\big] = b_{00}+b_{11}$ expressed in Eq. (18). From these two matrices for $\mathcal{S}_{00}(\rho)$ and $\mathcal{S}_{01}(\rho)$, the joint state $\mathcal{S}(\rho\otimes\rho_c)$ of Eq. (3) for the probe-control qubit pair of the switched channel can be represented as the 4×4 matrix

$$\mathcal{S}(\rho\otimes\rho_c) = \begin{bmatrix} p_c\mathcal{S}_{00}(\rho) & \sqrt{(1-p_c)p_c}\,\mathcal{S}_{01}(\rho) \\ \sqrt{(1-p_c)p_c}\,\mathcal{S}_{01}(\rho) & (1-p_c)\mathcal{S}_{00}(\rho) \end{bmatrix}. \tag{A-6}$$

As mentioned at the beginning of Section 4, if only the probe qubit, that interacts with the unitary U_ξ, is measured, then the performance for estimating the phase ξ is similar to a standard cascade, with standard properties. Meanwhile, if only the control qubit, that does not directly interact with the unitary U_ξ, is measured, then non-standard performance results, with non-standard properties inaccessible to standard estimation, as analyzed in Section 4. If the two qubits, probe and control, of the switched channel, are measured for phase estimation, the resulting performance can be analyzed by means of the joint state $\mathcal{S}(\rho\otimes\rho_c)$ characterized in Eq. (A-6). An

eigendecomposition of this bipartite state $\mathcal{S}(\rho \otimes \rho_c)$ would give access to its four eigenstates $|\lambda_\ell\rangle$ and four eigenvalues λ_ℓ determining [32,22] the quantum Fisher information

$$F_q(\xi) = 2\sum_{\ell=1}^{4}\sum_{m=1}^{4}\frac{|\langle\lambda_\ell|\partial_\xi \mathcal{S}(\rho\otimes\rho_c)|\lambda_m\rangle|^2}{\lambda_\ell+\lambda_m} \tag{A-7}$$

characterizing the performance upon measuring the qubit pair for estimating the phase ξ. This, however, can hardly be accomplished analytically in general, and preclude the accessibility of closed-form analytical solutions as they were obtained in Section 4 for the control qubit. Alternatively, numerical analysis can be implemented, with however a rather large range of configurations to be explored, according to the noise parameters (p, γ), the input configuration of the qubit pair and its output measurement. A combination of the standard and non-standard properties can be expected to hold. Such two-qubit approaches and their optimization remain open for further characterization.

References

[1] O. Oreshkov, F. Costa, Č. Brukner, Quantum correlations with no causal order, Nat. Commun. 3 (2012) 1092.
[2] G. Chiribella, G.M. D'Ariano, P. Perinotti, B. Valiron, Quantum computations without definite causal structure, Phys. Rev. A 88 (2013) 022318.
[3] L.M. Procopio, A. Moqanaki, M. Araújo, F. Costa, I.A. Calafell, E.G. Dowd, D.R. Hamel, L.A. Rozema, Č. Brukner, P. Walther, Experimental superposition of orders of quantum gates, Nat. Commun. 6 (2015) 7913.
[4] G. Rubino, L.A. Rozema, A. Feix, M. Araujo, J.M. Zeuner, L.M. Procopio, Č. Brukner, P. Walther, Experimental verification of an indefinite causal order, Sci. Adv. 3 (2017) e1602589.
[5] K. Goswami, C. Giarmatzi, M. Kewming, F. Costa, C. Branciard, J. Romero, A.G. White, Indefinite causal order in a quantum switch, Phys. Rev. Lett. 121 (2018) 090503.
[6] K. Wei, N. Tischler, S.-R. Zhao, Y.-H. Li, J.M. Arrazola, Y. Liu, W. Zhang, H. Li, L. You, Z. Wang, Y.-A. Chen, B.C. Sanders, Q. Zhang, G.J. Pryde, F. Xu, J.-W. Pan, Experimental quantum switching for exponentially superior quantum communication complexity, Phys. Rev. Lett. 122 (2019) 120504.
[7] Y. Guo, X.-M. Hu, Z.-B. Hou, H. Cao, J.-M. Cui, B.-H. Liu, Y.-F. Huang, C.-F. Li, G.-C. Guo, G. Chiribella, Experimental transmission of quantum information using a superposition of causal orders, Phys. Rev. Lett. 124 (2020) 030502.
[8] D. Ebler, S. Salek, G. Chiribella, Enhanced communication with the assistance of indefinite causal order, Phys. Rev. Lett. 120 (2018) 120502.
[9] L.M. Procopio, F. Delgado, M. Enríquez, N. Belabas, J.A. Levenson, Communication enhancement through quantum coherent control of N channels in an indefinite causal-order scenario, Entropy 21 (2019) 1012.
[10] L.M. Procopio, F. Delgado, M. Enríquez, N. Belabas, J.A. Levenson, Sending classical information via three noisy channels in superposition of causal orders, Phys. Rev. A 101 (2020) 012346.
[11] N. Loizeau, A. Grinbaum, Channel capacity enhancement with indefinite causal order, Phys. Rev. A 101 (2020) 012340.
[12] G. Chiribella, Perfect discrimination of no-signalling channels via quantum superposition of causal structures, Phys. Rev. A 86 (2012) 040301(R).
[13] S. Koudia, A. Gharbi, Superposition of causal orders for quantum discrimination of quantum processes, Int. J. Quantum Inf. 17 (2019) 1950055.
[14] M. Frey, Indefinite causal order aids quantum depolarizing channel identification, Quantum Inf. Process. 18 (2019) 96.
[15] C. Mukhopadhyay, M.K. Gupta, A.K. Pati, Superposition of causal order as a metrological resource for quantum thermometry, arXiv:1812.07508 [quant-ph], 2018 (5 pages).
[16] X. Zhao, Y. Yang, G. Chiribella, Quantum metrology with indefinite causal order, Phys. Rev. Lett. 124 (2020) 190503.
[17] F. Chapeau-Blondeau, Noisy quantum metrology with the assistance of indefinite causal order, Phys. Rev. A 103 (2021) 032615.
[18] V. Giovannetti, S. Lloyd, L. Maccone, Quantum metrology, Phys. Rev. Lett. 96 (2006) 010401.
[19] V. Giovannetti, S. Lloyd, L. Maccone, Advances in quantum metrology, Nat. Photonics 5 (2011) 222–229.
[20] G.M. D'Ariano, C. Macchiavello, M.F. Sacchi, On the general problem of quantum phase estimation, Phys. Lett. A 248 (1998) 103–108.
[21] W. van Dam, G.M. D'Ariano, A. Ekert, C. Macchiavello, M. Mosca, Optimal quantum circuits for general phase estimation, Phys. Rev. Lett. 98 (2007) 090501.
[22] F. Chapeau-Blondeau, Optimized probing states for qubit phase estimation with general quantum noise, Phys. Rev. A 91 (2015) 052310.
[23] C.L. Degen, F. Reinhard, P. Cappellaro, Quantum sensing, Rev. Mod. Phys. 89 (2017) 035002.
[24] A.G. de Oliveira, R.M. Gomes, V.C.C. Brasil, N. Rubiano da Silva, L.C. Céleri, P.H. Souto Ribeiro, Full thermalization of a photonic qubit, Phys. Lett. A 384 (2020) 126933.
[25] S. Khatri, K. Sharma, M.M. Wilde, Information-theoretic aspects of the generalized amplitude-damping channel, Phys. Rev. A 102 (2020) 012401.
[26] B.J. Falaye, A.G. Adepoju, A.S. Aliyu, M.M. Melchor, M.S. Liman, O.J. Oluwadare, M.D. González-Ramírez, K.J. Oyewumi, Investigating quantum metrology in noisy channels, Sci. Rep. 7 (2017) 16622.
[27] W.K. Tham, H. Ferretti, A.V. Sadashivan, A.M. Steinberg, Simulating and optimising quantum thermometry using single photons, Sci. Rep. 6 (2016) 38822.
[28] S.-C. Wang, Z.-W. Yu, W.-J. Zou, X.-B. Wang, Protecting quantum states from decoherence of finite temperature using weak measurement, Phys. Rev. A 89 (2014) 022318.
[29] M.A. Nielsen, I.L. Chuang, Quantum Computation and Quantum Information, Cambridge University Press, Cambridge, 2000.
[30] N. Gillard, E. Belin, F. Chapeau-Blondeau, Enhancing qubit information with quantum thermal noise, Physica A 507 (2018) 219–230.
[31] O.E. Barndorff-Nielsen, R.D. Gill, Fisher information in quantum statistics, J. Phys. A 33 (2000) 4481–4490.
[32] M.G.A. Paris, Quantum estimation for quantum technology, Int. J. Quantum Inf. 7 (2009) 125–137.
[33] P. Facchi, R. Kulkarni, V.I. Man'ko, G. Marmo, E.C.G. Sudarshan, F. Ventriglia, Classical and quantum Fisher information in the geometrical formulation of quantum mechanics, Phys. Lett. A 374 (2010) 4801–4803.
[34] F. Chapeau-Blondeau, Entanglement-assisted quantum parameter estimation from a noisy qubit pair: a Fisher information analysis, Phys. Lett. A 381 (2017) 1369–1378.
[35] F. Chapeau-Blondeau, Optimizing qubit phase estimation, Phys. Rev. A 94 (2016) 022334.
[36] D. Brivio, S. Cialdi, S. Vezzoli, B.T. Gebrehiwot, M.G. Genoni, S. Olivares, M.G.A. Paris, Experimental estimation of one-parameter qubit gates in the presence of phase diffusion, Phys. Rev. A 81 (2010) 012305.
[37] R. Okamoto, M. Iefuji, S. Oyama, K. Yamagata, H. Imai, A. Fujiwara, S. Takeuchi, Experimental demonstration of adaptive quantum state estimation, Phys. Rev. Lett. 109 (2012) 130404.
[38] R. Demkowicz-Dobrzański, L. Maccone, Using entanglement against noise in quantum metrology, Phys. Rev. Lett. 113 (2014) 250801.
[39] F. Chapeau-Blondeau, Quantum parameter estimation on coherently superposed noisy channels, Phys. Rev. A 104 (2021) 032214.
[40] L. Gammaitoni, P. Hänggi, P. Jung, F. Marchesoni, Stochastic resonance, Rev. Mod. Phys. 70 (1998) 223–287.
[41] F. Chapeau-Blondeau, Noise-assisted propagation over a nonlinear line of threshold elements, Electron. Lett. 35 (1999) 1055–1056.
[42] M.D. McDonnell, N.G. Stocks, C.E.M. Pearce, D. Abbott, Stochastic Resonance: From Suprathreshold Stochastic Resonance to Stochastic Signal Quantization, Cambridge University Press, Cambridge, 2008.
[43] F. Duan, F. Chapeau-Blondeau, D. Abbott, Non-Gaussian noise benefits for coherent detection of narrowband weak signal, Phys. Lett. A 378 (2014) 1820–1824.
[44] J.J.L. Ting, Stochastic resonance for quantum channels, Phys. Rev. E 59 (1999) 2801–2803.
[45] G. Bowen, S. Mancini, Stochastic resonance effects in quantum channels, Phys. Lett. A 352 (2006) 272–275.
[46] F. Chapeau-Blondeau, Qubit state estimation and enhancement by quantum thermal noise, Electron. Lett. 51 (2015) 1673–1675.
[47] N. Gillard, E. Belin, F. Chapeau-Blondeau, Stochastic antiresonance in qubit phase estimation with quantum thermal noise, Phys. Lett. A 381 (2017) 2621–2628.
[48] N. Gillard, E. Belin, F. Chapeau-Blondeau, Stochastic resonance with unital quantum noise, Fluct. Noise Lett. 18 (2019) 1950015.
[49] R. Demkowicz-Dobrzański, J. Kolodyński, M. Gută, The elusive Heisenberg limit in quantum-enhanced metrology, Nat. Commun. 3 (2012) 1063.
[50] F. Chapeau-Blondeau, Optimized entanglement for quantum parameter estimation from noisy qubits, Int. J. Quantum Inf. 16 (2018) 1850056.
[51] M. Araújo, F. Costa, Č. Brukner, Computational advantage from quantum-controlled ordering of gates, Phys. Rev. Lett. 113 (2014) 250402.
[52] H. Kristjánsson, G. Chiribella, S. Salek, D. Ebler, M. Wilson, Resource theories of communication, New J. Phys. 22 (2020) 073014.